Volume 80, March 2014 ISSN 0010-938X

ELSEVIER

CORROSION SCIENCE

The Journal on Environmental Degradation of Materials and its Control

Editor-in-Chief: G. T. BURSTEIN, University of Cambridge, U.K.

An Official Journal of the Institute of Corrosion

CONTENTS

Contents continued on outside back cover

http://www.elsevier.com/locate/corsci

Corrosion Science 80 (2014) 290–298

Contents lists available at ScienceDirect

Corrosion Science

journal homepage: www.elsevier.com/locate/corsci

Pitting corrosion of cold rolled solution treated 17-4 PH stainless steel

Davood Nakhaie, Mohammad Hadi Moayed *

Department of Materials and Metallurgical Engineering, Faculty of Engineering, Ferdowsi University of Mashhad, Mashhad 91775-1111, Iran

ARTICLE INFO

Article history:
Received 17 April 2013
Accepted 26 November 2013
Available online 4 December 2013

Keywords:
A. Stainless steel
B. Polarization
C. Effects of strain
C. Pitting corrosion

ABSTRACT

In the present paper the effects the of cold rolling on pitting corrosion of 17-4 precipitation hardening stainless steel in 3.5 wt% NaCl solution was investigated. In order to clarify the effect of cold rolling the metastable pitting has been examined in more details. The results presented show that cold rolling increases the dissolution rate of metastable pitting in a manner which facilitates the transition from metastable to stable pitting. On the other hand, the frequency of occurrence of metastable pits decreases with cold working. In overall, cold rolling has no significant effect on pitting potential.

1. Introduction

The plenitude of applications has made the stainless steels important classes of alloys. For many applications, stainless steels are subjected to different levels of cold working during the final steps of manufacturing. In practical point of view, beside of the corrosion resistance, the mechanical properties of stainless steels are of interest. In the annealed state, yield strength of austenitic stainless steels is relatively low. Higher yield strength and tensile strength can be achieved through cold working process. Such improvement in mechanical properties by plastic deformation generally accompanies with microstructural changes like increasing dislocations density, introducing deformation bands, twining, and more importantly for austenitic stainless steels, deformation induced martensite [1–3]. Microstructure is one of the most important metallurgical aspects of localized corrosion of stainless steels. So that, the influence of cold working on corrosion resistance of stainless steels has been subject of several studies [1–10]. However, no comprehensive model has been proposed on the influence of cold plastic deformation on localized corrosion of stainless steels. While it has shown that cold rolling decreases the pitting potential of austenitic stainless steels [2,3,5,10], on contrast, increase in pitting potential of work-hardened stainless steel has also been observed [7]. Higher passive current and lower protection potential have been reported for cold worked stainless steels. It is also mentioned that pit propagation takes place easier for the work-hardened material [2,3]. However, lower passive current and more noble protection potential has been observed for the cold rolled stainless steel [7].

For an austenitic stainless steel, it has been shown that the number of pits generally increases with increasing pre-deformation. Moreover, the rate of pit growth increases even after small deformation (1%) but more severe deformation has little additional effect [10]. Both the thickness and Cr:Fe ratio of passive film on AISI 304 stainless steel increase as a result of cold rolling procedure. X-ray diffraction has shown a texture for cold rolled material, which enhances diffusion of Cr into the passive film over the surface and therefore, increases pitting resistance [7]. Susceptibility to pitting for AISI 304 stainless steel in chloride containing sulfate media was reported to be greater for cold worked than annealed sample. The in situ microscopic observation has showed that pit initiation began at defective interfaces. The passivity decay with cold rolling appeared to be mainly due to the formation of defective interfaces [2].

It has been reported that prior deformation accelerates the sensitization of stainless steels. Plastic deformation induces slip bands, which are prime sites for carbide precipitations. Cold working promotes the formation of both grain boundary and intragranular Cr_2N precipitates of a high-nitrogen stainless steel. On the other hand, desensitization was shown to be faster in highly cold worked material, especially at high temperatures [6,9].

Among microstructural changes occur during cold working, modification of non-metallic inclusions has an important role in both strip quality and corrosion resistance. Cold working may produce and elongate the inclusions or produce micro-cracks at the interface of matrix–inclusion, which affects the pitting resistance of stainless steel [11,12].

Passivity break down, which plays an important role in initiation of localized corrosion of stainless steels, is a phenomenon showing a statistical and probabilistic nature [13,14]. Even at controlled laboratory conditions, passivity breakdown exhibits a wide

* Corresponding author. Tel.: +98 5118763305; fax: +98 5118763301.
E-mail address: mhmoayed@um.ac.ir (M.H. Moayed).

0010-938X/$ - see front matter © 2013 Elsevier Ltd. All rights reserved.
http://dx.doi.org/10.1016/j.corsci.2013.11.039

scatter of initiation time and/or location on the electrode surface. Therefore, the pitting potential may not be considered as a unique value determined for a given combination of material and environment. Although the importance of the probabilistic nature of the potential at which a stable pit forms has been well acknowledged, to our knowledge, no attempt has been made so far to employ statistic/stochastic approaches to pitting phenomena in matter of cold worked stainless steels. Assessment of the influence of cold working on the pitting corrosion by using statistical approach may lead to more in-depth understanding.

The 17-4 PH stainless steel is one of most common types of precipitation hardening stainless steels. The combination of high strength and ductility together with moderate corrosion resistance has made this steel an attractive material for designers [15–19]. In the present investigation the effect of cold rolling on pitting corrosion of solution treated 17-4 PH stainless steel in 3.5 wt% NaCl solution was studied. Although this stainless steel is not used in solution treated condition, however, it is still worth to study the influence of cold working on its pitting corrosion susceptibility. Attempt has been made to explain the effect of cold working using statistical approach with emphasis on pitting initiation.

2. Experimental

2.1. Material and cold rolling

The 17-4 PH (UNS S17400) stainless steel was supplied by EICO, Esfarayen, Iran. The material was received as a hot rolled billet with diameter of 90 mm. The alloy composition is given in Table 1. Discs with 5 mm thickness were obtained from the billet and were solution treated at 1050 °C for 1 h and then were water quenched. By this solution heat treatment the previous Cu-rich precipitates dissolve and the martensitic matrix supersaturates with Cu and Cr [17]. Solution treated discs were subjected to cold rolling leading to 10%, 30%, 50% and 70% final reduction of thickness. For the rest of the paper, specimens are denoted as ST for solution treated, 10%, 30%, 50% and 70% for 10%, 30%, 50% and 70% cold rolled specimens, respectively. 10 mm × 10 mm specimens were cut from the rolled discs, with test surfaces parallel to the rolling direction. Then the specimens were mounted into epoxy resin, polished up to diamond finish (1 μm), and etched in modified Fry's reagent to reveal the microstructural changes due to the cold rolling [20]. Microstructure of the solution treated and the cold rolled samples was examined using optical microscopy and scanning electron microscopy (SEM) equipped with energy dispersive X-ray spectrometry (EDX).

2.2. Potentiodynamic experiments

Potentiodynamic experiments were carried out in three-electrode cell at two different potential scan rates of 30 and 5 mV/min in 3.5 wt% NaCl solution. Higher potential scan rate was employed to investigate the effect of cold rolling on pitting potential, and slower potential scan rate was used to study the nucleation frequency of metastable pitting as a function of cold working. The electrochemical cell was a 250 ml beaker open to air. A saturated Calomel electrode (SCE) as reference electrode and a platinum wire as counter electrode were used. The exposed surface area of 0.5 and 0.2 cm^2 was prepared for the higher and lower potential scan rates, respectively. The electrodes surface was prepared by grinding up to 1200 grit SiC paper. For all experiments, the polarization started after 15 min recording corrosion potential, which was enough to approach steady state condition. All experiments were performed at room temperature, and were repeated 15 times at higher potential scan rate and 5 times at lower potential scan rate.

2.3. Potentiostatic experiments

To study pit nucleation, potentiostatic experiments were carried out at constant potential of 0 V/SCE. Surface area of 0.2 cm^2 of each sample, which was finished with 1200 grit SiC paper, was exposed to the 3.5 wt% NaCl solution open to air. Such surface area was chosen to reduce the overlap of events. Before the test beings run, open circuit potential was measured for 15 min, and then current response of the sample at constant potential was recorded at frequency of 50 Hz for 1200 s. All experiments were carried out at room temperature and were repeated 5 times for each specimen.

3. Experimental results

3.1. Microstructure

Fig. 1 shows the microstructure of 17-4 PH stainless steel after solution heat treatment at 1050 °C for 1 h. The microstructure was composed mainly of martensite and minor fraction of δ-ferrite (less than 1%). It has been shown that the martensite at this condition consists of lath structure containing very high density of dislocations [17]. No evidence of Cu-rich precipitates in the matrix has been observed in the solution treated condition and it is believed that the martensite is supersaturated with Cu and Cr [16,17]. The absence of δ-ferrite in the microstructure allows considering the effect of cold rolling only on the martensite phase.

Fig. 2a shows SEM micrograph of an inclusion in specimen 10%. The EDX analysis, Fig. 2b, indicates that the inclusion is sulfide type and contains Fe and Cr. When the steel is subjected to cold deformation, because the non-metallic inclusions and the steel matrix have different ductility, the applied strain creates a trench at the interface of matrix and inclusion. Such trench is shown in Fig. 2c and d for specimens 50% and 70%, respectively. By increasing the cold working the fracture at the interface has occurred more severely. In specimen 70%, for example, the inclusion is nearly debonded from the matrix. Beside the inclusion, Fig. 2c shows some spherical precipitates. The EDS analysis has indicated that they are Nb-rich phases and are believed to be NbC carbides [21].

3.2. Pitting potential

Typical potentiodynamic polarization curves obtained in 3.5% NaCl solution at 25 °C for different specimens are depicted in Fig. 3. As it can be seen, cold rolling did not noticeably influence the corrosion potential and the passivity current density. Since pitting potential (E_{pit}) has a probabilistic character [20], it is reasonable to employ statistical approach to address the effect of plastic deformation on E_{pit}.

Fig. 4 shows the cumulative probability of pitting potential distribution for 17-4 PH stainless steel with different cold rolling reductions determined from potentiodynamic polarizations. The

Table 1
Chemical composition (in weight percent) of 17-4 PH stainless steel.

C	S	P	Si	Mn	Cu	Ni	Cr	V	Nb	Mo	Fe
0.04	0.012	0.018	0.32	0.61	4.14	4.59	15.09	0.013	0.358	0.18	Bal.

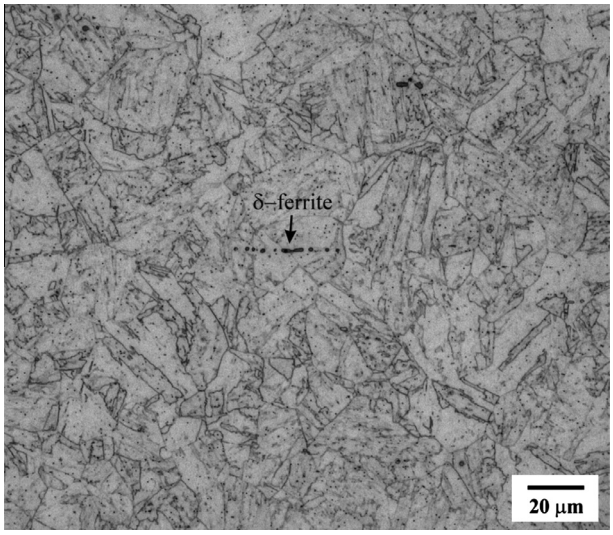

Fig. 1. Microstructure of 17-4 PH stainless steel after solution heat treatment at 1050 °C for 1 h, etched in modified Fry's reagent.

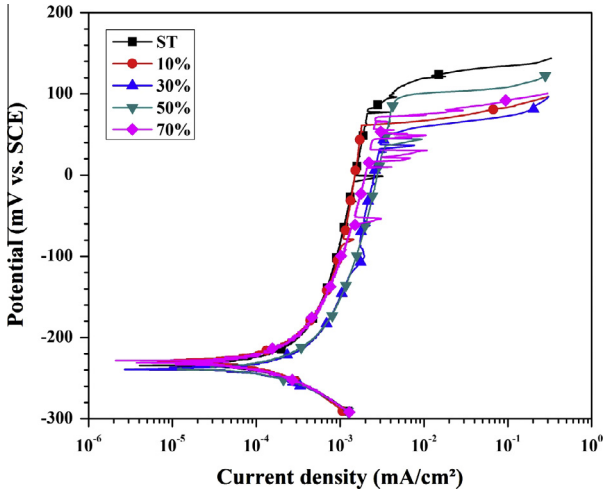

Fig. 3. Potentiodynamic polarization curves of 17-4 PH stainless steel obtained at potential scan rate of 30 mV/min in 3.5% NaCl at 25 °C for different levels of cold rolling.

graph represents the pitting probability, $P(E)$, as a function of potential, expressed as:

$$P(E) = \frac{n}{1+N} \quad (1)$$

where N is the total number of experiments and n is the number of pitted ones. The pitting potential distribution of a stainless steel strongly depends on the chosen current threshold at which it is thought that the pitting corrosion proceeds [22]. Current threshold values of 20 μA [13], 50 μA [23] and 200 μA [24] has been proposed for onset of pitting corrosion. In the present study, reaching current density of 100 μA/cm^2, equal to 50 μA considering the electrodes surface area of 0.5 cm^2, is taken into account as current threshold for determining pitting potential. None of the pits with a current density of 100 μA/cm^2 were repassivated.

Generally, the solution treated sample has the most positive values of E_{pit} distribution, while 30% cold rolled sample has the lowest E_{pit} distribution. The pitting potentials for 10%, 50% and 70% are distributed between the values of two other specimens. However, the E_{pit} of ST and 30% range from 95 to 178 mV/SCE and from 57 to 148 mV/SCE, respectively.

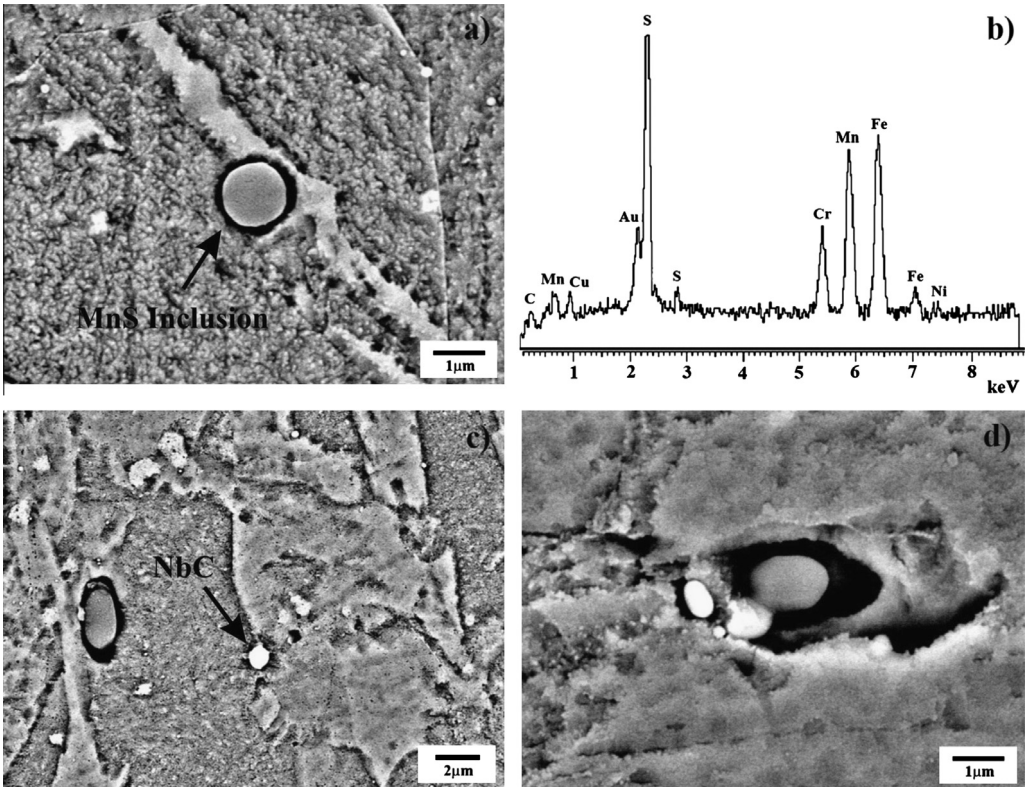

Fig. 2. Scanning electron micrograph of cold rolled specimens, etched in modified Fry's reagent: (a) specimen 10%, (b) EDS analysis of the MnS inclusion, (c) specimen 50%, and (d) specimen 70%.

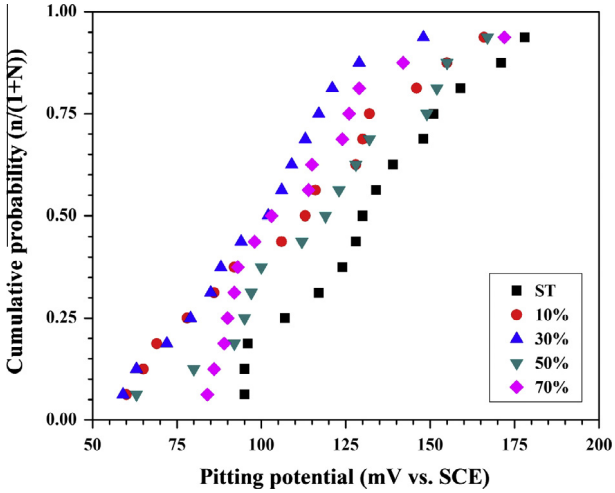

Fig. 4. Cumulative probability of pitting potential for different specimens.

In order to compare pitting potential of specimens with different levels of cold working, one may consider the median values of pitting probability, i.e. $P(E) = 0.5$. Solution treated specimen has the highest median E_{pit} and the lowest median E_{pit} belongs to 30%. However, their difference is only 32 mV/SCE, which is less than the difference between the maximum and the minimum values of pitting potential of ST (83 mV/SCE). Therefore, it can be concluded that the cold rolling did not noticeably alter the pitting potential of 17-4 PH stainless steel.

3.3. Metastable pitting

Fig. 5 illustrates the typical current transients obtained from the potentiostatic polarization of solution treated 17-4 PH stainless steel in 3.5% NaCl solution. There are many current spikes lay over the background passive current. These events are characterized by increasing the current from passivity background as the pit nucleates and beings to grow. After a short time of growth, by rupture of the cover over the pit mouth and dilution of the pit solution, the metastable pit repassivates, and consequently, the current suddenly decreases to the original value of passive current [25,26]. However, another type of current transients has been reported, progressive increase and decrease of the current [27]. In the present study, both kinds of transients have been observed. Fig. 6 shows current transients of two metastable pits developed on ST and graphically represents the key characteristics of these transients, i.e. the pit peak current (I_{peak}), pit growth time (t_g) and pit repassivation time (t_r).

Fig. 7 shows the cumulative probability plot of I_{peak} for different specimens. I_{peak} is taken as the difference between the maximum current measured in a transient and the background noise in potentiostatic experiment. To draw the diagram, 30 I_{peak} of more than 150 transients for each specimen were chosen randomly. Also, Eq. (1) was used as the cumulative distribution function. As it can be seen, the peak current of metastable pits increases as the cold rolling increased. For ST, which shows the lowest values of peak current, the median of I_{peak} is 97 nA. 10% cold rolling has small effect on the peak current. However, by increasing the plastic deformation to 30%, the median of I_{peak} increases to 180 nA. The median of distribution of I_{peak} for 50% and 70% are 4 times and 6 times more than ST, respectively. Although the pit peak current of specimens ST and 10% are less than 400 and 520 nA, respectively, specimen 50% and in particular 70%, possess metastable pits greater than 1 μA.

Fig. 8 illustrates the cumulative probability of metastable pits growth time for different levels of cold rolling. The t_g is taken as the difference between the moment that the current began to increase as the pit nucleates and the moment it starts to decrease as the pit begins to repassivate. As Fig. 8 shows, the growth time of metastable pits increases by increasing the cold rolling. Metastable pits occurred on the surface of the specimen 10% have just slightly longer growth times than that of ST, which possesses the shortest t_g. Metastable pits developed on 30% have more extended growth times. The specimens 50% and 70% even have longer growth time which their median distribution of t_g is 3.7 times and 5.4 times longer than that of ST, respectively.

The cumulative distribution of growth rate of metastable pits of 17-4 PH stainless steel at different cold rolling degrees is shown in Fig. 9. The growth rate is defined as the rate which a metastable pit reaches to its maximum radius just before repassivation and is calculated by dividing the pit peak current to the pit growth time [28]. The ST shows the least metastable pits growth rate. By increasing the cold rolling the growth rate of metastable pits is increased. Despite the fact that more plastic deformation results in higher pit currents and more extended growth times (Figs. 7 and 8), the metastable pits growth rate increased. For instance, even though specimen 70% possesses the greatest values of I_{peak} and t_g among

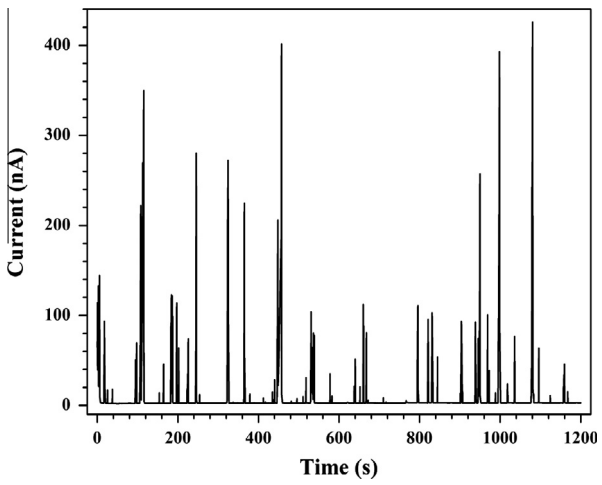

Fig. 5. Current transients from metastable pitting of solution treated 17-4 PH stainless steel at 0 V/SCE in 3.5% NaCl solution at 25 °C.

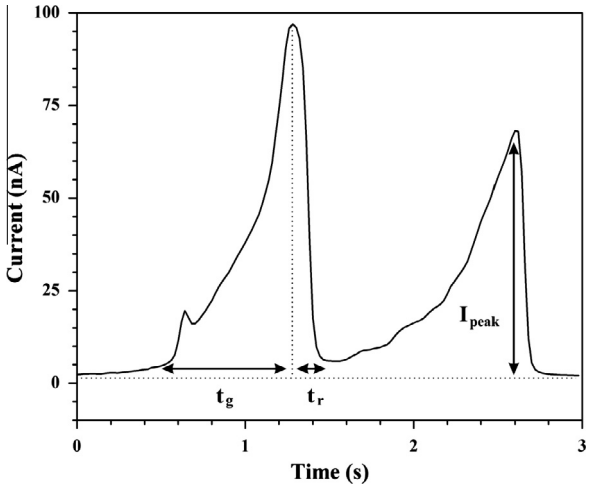

Fig. 6. Typical current transients of solution treated 17-4 PH stainless steel at 0 V/SCE in 3.5% NaCl solution at 25 °C.

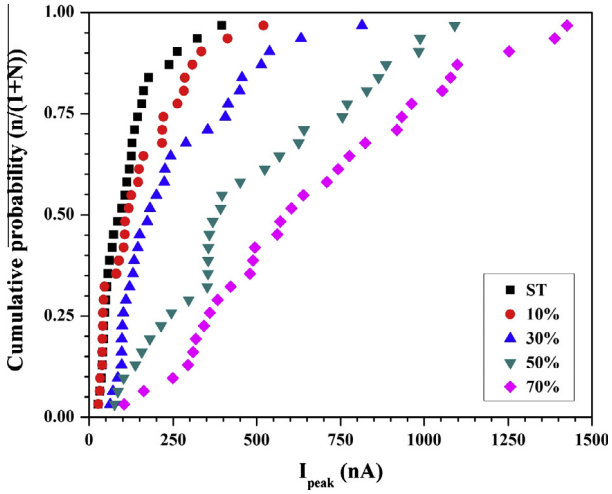

Fig. 7. Cumulative probability of metastable pit peak current for different specimens.

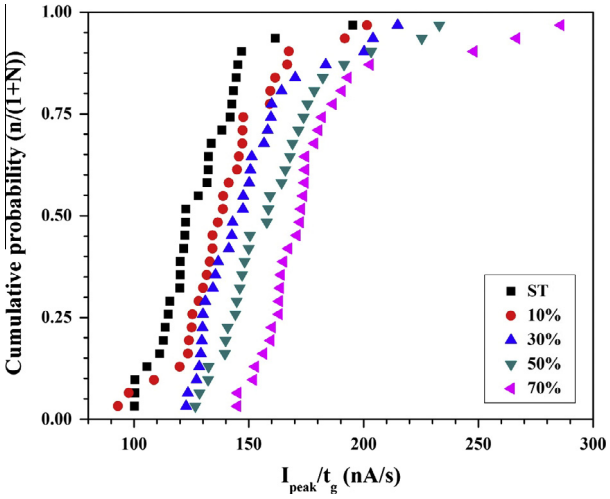

Fig. 9. Cumulative probability of metastable pit growth rate for different levels of cold rolling.

other specimens, the rate of metastable pits growth of this specimen is still highest. This implies that the effect of cold rolling on increasing the pit peak current was more pronounced than that of pit growth time.

Fig. 10 depicts the cumulative distributions of repassivation time of metastable pits for different specimens. As with growth time, cold rolling lingered repassivation time of metastable pits. However, such lengthening in repassivation time is less strict than growth time. For instance, the median of repassivation time of 70% is 3.8 times greater than that of ST, whilst its median growth time is 5.4 times more than that of ST. In addition, metastable pits of ST, for example, repassivate less than 0.26 s, while the least pit growth time of this specimen is 0.32 s. Regardless of plastic deformation state, comparison between the median of growth time and repassivation time it reveals that the majority of metastable pits developed on 17-4 PH stainless steel repassivate much faster than they grow.

The apparent radius of each metastable pit was calculated from total anodic charge of the pit by utilizing Faraday's law on the assumptions that the growing pit was hemisphere. It has been shown that assuming a growing metastable pit as a hemisphere is acceptable [25]. It is also assumed that the mean oxidation state of alloy was 2.19 per mole, the density was 7.82 g/cm^3 and the molar mass of the alloy was 56.2 g/mole. Fig. 11 illustrates the cumulative distribution of calculated metastable pit radii (r_{pit}) for different specimens. The radius of metastable pits of ST is ranged from 0.41 to 0.82 μm with median of distribution of 0.52 μm. By increasing the cold deformation the radii of hemispheres is also increased. Metastable pits on specimen 10% are just bigger than those on ST. Specimen 30% has even larger metastable pits. Increasing the cold rolling to 70% increases the median of distribution to 1.68 μm.

According to Galvele [29], for a unidirectional pit with depth of a and current density of i, the product of $i.a$ have to exceed a certain critical value to pit grow stably. The product of $i.a$, which is known as pit stability product, can be used to evaluate the susceptibility of formation of stable pits [25,30]. The stability products were calculated using the metastable pit current density just before repassivation multiplying to the pit apparent radius and compared for ST and cold rolled specimens in Fig. 12. The current density of a metastable pit is nearly constant with time [25,31], therefore, the current density of pit before the pit death can be considered as the current density throughout the pit growth. Higher pit current density and higher pit radius results in higher pit stability product.

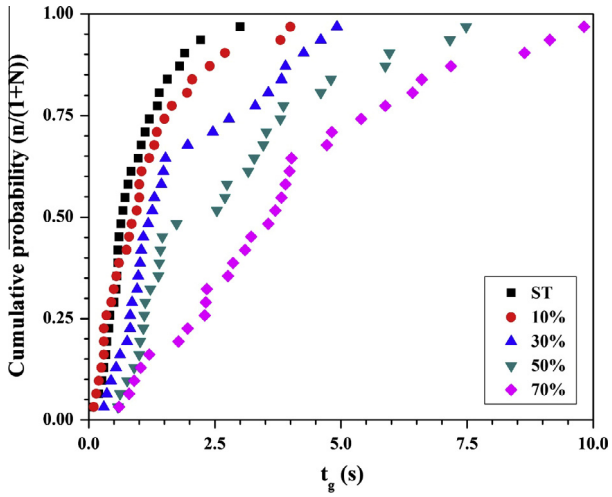

Fig. 8. Cumulative probability of metastable pit growth time for different specimens.

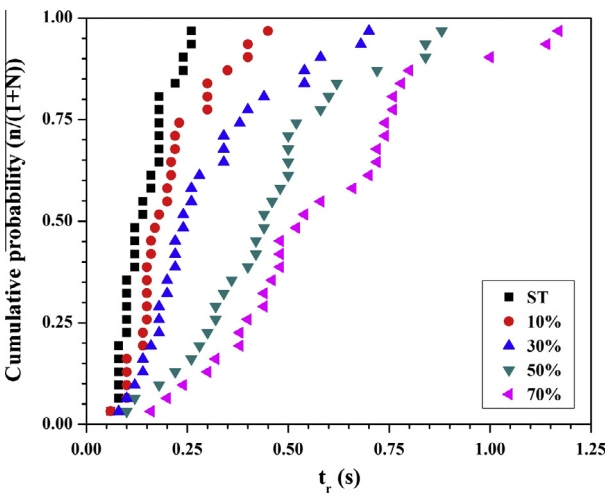

Fig. 10. Cumulative probability of metastable pit repassivation time for different specimens.

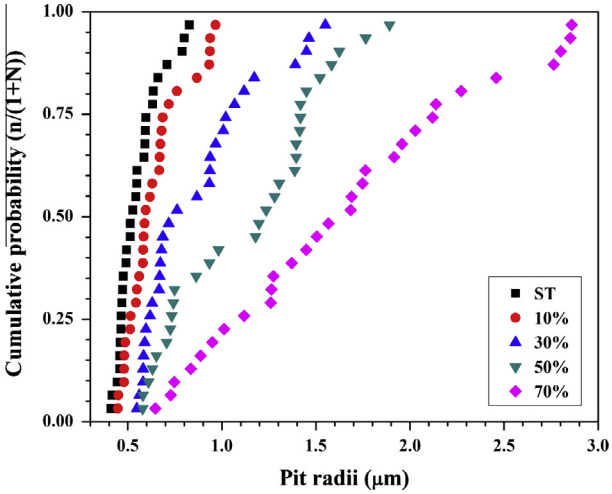

Fig. 11. Cumulative probability of metastable pit radii (calculated at I_{peak}) for different specimens.

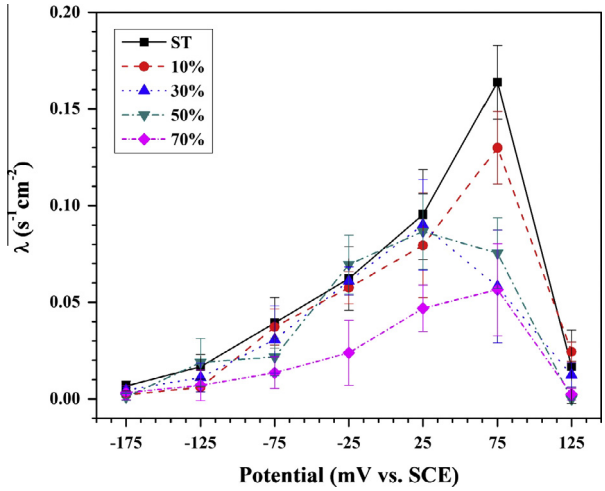

Fig. 13. Metastable pitting occurrence of 17-4 PH stainless steel as a function of potential during potentiodynamic polarization at scan rate of 5 mV/min. Each data point represents the average frequency of events calculated from 5 separate runs and is presented at the middle of 50 mV interval; Error bars give the 95% confidence interval.

Cold rolling significantly increased the stability product of metastable pits. The stability product of ST is ranged from 0.12 to 0.45 mA/cm, while, the minimum stability product of 30% is 0.41 mA/cm. Fig. 12 clearly shows that the stability products of specimens 50% and especially 70% are far greater than that of ST.

3.4. Metastable pitting initiation

The rate of pit initiation (λ) was showed that is proportional to the applied potential [32]. The pit initiation rate, which is the frequency of pit initiation per unit time, is given by:

$$\lambda(t) = -\frac{\mathrm{d}\ln P(t)}{\mathrm{d}t} \tag{2}$$

where $P(t)$, or survival probability, is the proportion of non-pitting specimens at the time t. The survival probability is expressed as:

$$P(t) = 1 - P(E) = 1 - \frac{n}{1+N} \tag{3}$$

The average frequencies of metastable pit occurrence as a function of applied potential for different cold rolled specimens in 3.5% NaCl solution at potential scan rate of 5 mV/min are depicted in Fig. 13. The λ was obtained by counting the numbers of events within 50 mV intervals of potential sweep and dividing by the time taken to traverse that interval (600 s at a sweep rate of 5 mV/min) and dividing by 0.2 cm^2 (electrode surface area). It should be noted that all events greater than 3 nA were considered as metastable pit. Each data point in Fig. 13 represents the average frequency of events calculated from 5 separate runs and is presented at the middle of 50 mV interval. For all specimens λ rises as the potential increases until reaching a maximum value, and then, sharply decreases. Similar behavior of increase and decrease of λ has been reported by other researchers [25,33]. However, they observed that the frequency of metastable pitting increases rapidly to a maximum and then decreases gradually. The decrease of λ at more anodic potentials is believed to be the result of the elimination of pit nucleation sites from the electrode surface [25,34].

The potential interval at which the maximum metastable pitting occurred for specimens ST, 10% and 70% is 50–100 mV and specimens 30% and 50% reached the maximum λ at 0–50 mV interval. At lower potential intervals some overlaps can be seen for metastable pitting frequency of all specimens except specimen 70%, which at all potential intervals shows the least values of λ. Generally, by increasing the cold rolling the frequency of metastable pitting decreases. Considering the λ as the rate of metastable pitting, it is implied from Fig. 13 that cold working hinders the occurrence of these events.

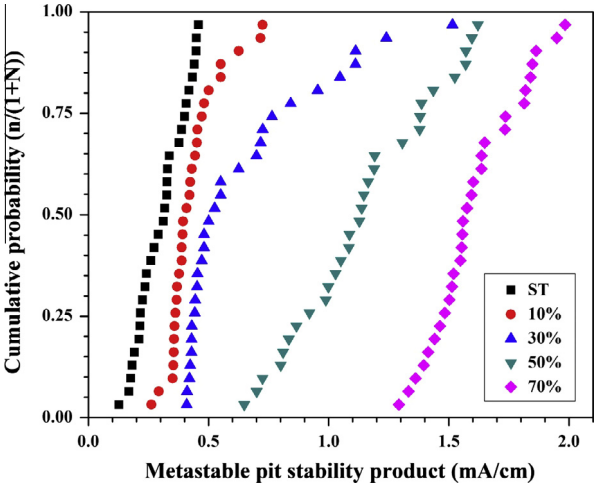

Fig. 12. Cumulative probability of metastable pit stability product for different specimens.

4. Discussion

In the present study two distinct effects of cold deformation on pitting corrosion of 17-4 PH stainless steel has been demonstrated: the first is the increase of dissolution kinetics as a function of cold rolling, and the second is the decrease of metastable pitting occurrence frequency by cold working. The combination of these two effects on pitting susceptibility was examined by means of pitting potential measurements.

4.1. Microstructure

Generally, the microstructure of the 17-4 PH stainless steel is largely composed of martensite and some amounts of δ-ferrite, which strongly depends on the steel chemical composition and its thermal or thermomechanical history. The presence of δ-ferrite

not only increases the heterogeneity of the steel, but also can significantly alter the mechanical properties of the material [15]. The investigating 17-4 PH stainless steel is mostly consisted of martensite, so that it can be considered as a single phase material. Therefore, the effect of cold rolling was studied only on the martensite.

The non-metallic inclusions play an important role on both mechanical behavior and pitting corrosion resistance of stainless steels [35]. Inclusion size, inclusion position, rolling speed and rolling reduction ratio are the most influential parameters affect the inclusion deformation within a cold rolled steel [11,12]. Assuming spherical shaped non-metallic inclusion, simulation using finite element method of cold rolled stainless steel has been shown that the strain value of the inclusion is much less than of the matrix [12]. During cold rolling, when non-uniform deformation takes place between the matrix and the inclusion micro-cracks might appear at the matrix–inclusion interface, especially in front of the inclusion where large strain values exists. The deformation of a inclusion decreases with decreasing the inclusion size, insomuch when the inclusion size is less than 10 μm, the strain difference between the matrix and inclusion causes crack formation [12]. It is also reported that the formation of crack in stainless steels under plastic deformation is associated with MnS inclusion. Tensile plastic deformation of a stainless steel produces formation of micro-cracks at the interface of matrix and irregular shaped MnS inclusion [11].

Fig. 2 shows decohesion of the matrix–inclusion interface of cold rolled specimens. Interface debonding increased by increasing plastic deformation. The micro-cracks formed between the matrix and the MnS inclusions in cold rolled specimens had remarkable importance in pitting initiation.

4.2. Effect of cold rolling on metastable pitting

Cold plastic deformation increases the dissolution kinetics of 17-4 PH stainless steel in 3.5% NaCl solution (Figs. 7–12). The main parameters have been affected by cold rolling are the metastable pit peak current and the metastable pit growth time. Although cold rolling increased both parameters, increment of pit peak current was more pronounced so that the growth rate of metastable pits is also increased by increasing the cold rolling level.

Pitting initiation in the stainless steels is closely related to the passive film stability and the presence of non-metallic inclusions. It is shown that cold working may weaken [2,3,5] or, on the contrary, strengthen the passive film [7]. Formation of defected interfaces because of the accumulation of internal stresses during the mechanical process is known to be responsible of passivity decay of cold deformed steel [2]. Examination of the microstructure of cold worked steels using transmission electron microscopy (TEM), electron diffraction and X-ray diffraction characterized the dislocation density, presence of deformation bands, slip bands and deformation induced martensite [1,3,4]. The density of dislocations increases considerably during the cold working. Planar deformation structure at lower cold rolling levels and cellular structure at higher reductions has been observed. Such planar structure is shown to increases the number of pits formed on steel surface [3]. Stain-induced martensite is believed to deteriorate pitting corrosion resistance of cold worked austenitic stainless steels [36]. In contrast, no direct effect on pitting susceptibility of the cold rolled stainless steel with the presence of deformation-induced martensite has been observed [3,7,37]. TEM analysis has been represented that the dislocations have an important effect on pitting susceptibility of stainless steels. Although the dislocation density of martensite phase is naturally quite high, TEM investigation of cold rolled martensitic steel is revealed that 11% plastic deformation increases the dislocation density more than 23 times compare to as quenched sample [8]. Since the 17-4 PH stainless steel used in the present study is martensitic, austenite to martensite transformation during cold rolling did not take place. However, it is expected that cold rolling increases the dislocation density of the steel, which is approximately $4 \times 10^{15}\ m^{-2}$ in solution annealed condition [38].

Since the growth rate of the metastable pits increases with increasing the deformation, once the passive film broke down the rate of dissolution of these specimens would be greater. In other words, the ability to repassivate the growing metastable pits decreased as increasing the cold rolling.

4.3. Metastable pitting initiation

Fig. 13 provides that the rate of metastable pitting is decreased by increasing cold rolling level. This can arise either because there were less available sites on the surface of cold worked specimens, or there were same number of sites, but they activated at slower rate. It has been shown that the number of available metastable pit sites on a stainless steel decay exponentially with time [25].

Eklund has shown that the MnS inclusions are thermodynamically unstable above −100 mV/SHE. Since the corrosion potential commonly measured on passive stainless steels in chloride containing solutions is more noble, when the steel is left at its free corrosion potential the MnS inclusion will be polarized and begins to dissolve. Because of low electrical conductivity of the inclusion, the dissolution begins to start locally at the interface of matrix–inclusion. The dissolved MnS inclusion produces a crevice at the interface of matrix–inclusion, which promotes the dissolution process [39]. Dissolution of MnS inclusions in a stainless steel 10 s exposed to Cl^- containing solution at the open circuit potential has been indicated that inclusions can either dissolve partially or completely. Even though hydrolysis of dissolved MnS inclusion increases the concentration of Cl^- within the cavity, it would not be sufficient to prevent the repassivation of the bare metal surface [40].

Previously, it was shown that cold rolling causes formation of micro-cracks at the interface of matrix-MnS inclusions (Fig. 2). The debonding became more sever at higher reduction levels. It is also mentioned that before starting the potentiodynamic polarization each sample was left at its free corrosion potential for 15 min. During this time, which was enough to approach the steady state condition, the MnS inclusions start to dissolve non-uniformly establishing from matrix–inclusion interface [41]. The inclusions in the solution treated specimen begin to dissolve progressively during the immersion time by formation of crevice at the matrix–inclusion interface. On the other hand, the dissolution of inclusions in cold rolled samples proceeds even faster, because the cavity formed by cold rolling eases the dissolution of the inclusion. In other words, the kinetics of dissolution of MnS inclusions within cold worked specimens enhances by the formation of cavity at the matrix–inclusion interface. Since plastic deformation increased the cracking at the interface, the probability of complete dissolution of inclusions at the same immersion time increases. If consider the MnS inclusions as preferred sites for nucleation of metastable pits, when the steel was undergone the polarization, there were less number of available sites for metastable pitting occurrence. As a result, the metastable pitting frequency of 17-4 PH stainless steel decreased as the cold rolling increased. This interpretation is in agreement with those have been observed by other researchers. Stewart and Williams reported that laser surface melting by reducing the size of inclusions markedly decreases the nucleation rate of metastable pits [42]. Sudesh et al. have shown that by decreasing the sulfur content of the stainless steels and hence reducing the MnS inclusions the metastable pitting frequency decreases considerably [43].

4.4. Transition from metastability to stability

Cold plastic deformation of 17-4 PH stainless steel increases the current density of metastable pits. The intensification of the pit current density by cold rolling implies that the dissolution rate of metal increases. Therefore, the amount of metal free cations inside the pit increases and hence, the diffusion of Cl^- ions into the pit increases. The main result of the increase in the rate of metal dissolution in the pits by increasing cold rolling is that the sizes of metastable pits were increased correspondingly. As Fig. 11 clearly shows, the metastable pits formed on cold rolled specimens are much larger compared to ST. Increase in the pit depth (pit radius) increases the diffusion barrier of metal cations outside the pit [30]. As a result, it is expected that the concentration of metal cations inside the pit increases. To estimate the cations concentration within a growing pit Eq. (4) was proposed [25]:

$$\Delta C = \left(\frac{2\pi}{3zFD}\right) ia \tag{4}$$

where ΔC is the gradient of cations between pit interior and bulk solution, z is the mean oxidation state of cations (2.19), F is the Faraday's constant in C/mol, D is the diffusion coefficient (ca. 10^{-5} cm^2/s), i is the pit current density and a is the pit radius. The cations concentration for different specimens was calculated from the median of corresponding stability product distribution and is given in Table 2.

If it is assumed that the cation concentration in the bulk solution is zero, ΔC will be the cations concentration at the pit surface [25]. Table 2 shows that small amount of cations were dissolved in ST compared with work-hardened specimens. It has been shown that the concentration of metal cations have to be more than ca. 3 M to prevent repassivation of a growing pit [25]. Such critical metal cation concentration is equal to stability product of 3 mA/cm. From the cumulative distribution of metastable pit stability product illustrated in Fig. 12 it can be seen that pits of cold rolled specimens easier can attain the critical concentration. In other words, higher dissolution rate of metastable pits of cold rolled specimens makes it easier to achieve the minimum cation concentration needed for prevention of repassivation. As the dissolution rate increases with increasing cold rolling, this condition becomes more severe as well. For example, ΔC calculated from the median of stability product distribution for specimen 70 is equal to 1.56 M, which is more than half of the critical concentration. It worth to mention that in this specimen there were pits which have greater stability products and can reach stability even more easier.

4.5. Pitting potential

The initial growth stages of a metastable pit and a stable pit are almost similar. From kinetics point of view, in both cases the pit current density is nearly constant with time [25,27]. Williams et al. characterized the probability of formation of stable pits based on the rate of metastable occurrence and the probability of repassivation [44,45]. According to their work the relationship between metastable and stable pitting can be expressed as two probabilities: the probability of initiation of a metastable pit and transition probability from metastable to stable pit. Since the potential at which a stable pit forms has a probabilistic nature [14], the effect of cold rolling on pitting potential of 17-4 PH stainless steel can be argued. The data presented in this work shows that cold rolling decreases the number of metastable pits can be generated. The reduction of the rate of metastable pitting reduces the chance of formation of pits capable of attaining the critical pit stability product. On the other hand, metastable pits of cold rolled specimens experience higher rates of anodic dissolution, so that the attainment of minimum metal cation concentration required for stable growth will be easier. Accordingly, the cold rolling has a dual effect. While it increases the first probability, the latter probability decreases. Eventually, the product of these two probabilities resulted that the pitting potential for different specimens was almost same. The advantage of using statistical approach to pitting is that it gives brighter view of the effect of alloy or environment on pitting susceptibility. Although some researchers have considered less than 10 mV/SCE in pitting potential as the influence of cold working on stainless steels [3], the results of present study illuminates that the effect of cold plastic deformation on pitting potential of stainless steels needs broader survey. One possible explanation of the inconsistent results reported by different researchers for the influence of cold working on pitting corrosion resistance of stainless steels is that no attempt has been made to utilize statistical approach. However, by applying the methods explained in this paper it can be concluded that although cold rolling affects pitting initiation and transition from metastability to stability, the potential at which stable pits are formed is not influenced.

Table 2
Metal cation concentration inside the pits for different specimens calculated from the median of stability product distribution by using Eq. (4).

Specimen name	ST	10%	30%	50%	70%
ΔC (M)	0.315	0.405	0.520	1.126	1.561

5. Conclusion

1. Cold rolling formed micro-cracks at the interface of martensitic matrix and MnS inclusions of 17-4 PH stainless steel. The micro-cracks formed at the matrix–inclusion interface accelerate the dissolution of the inclusion during immersion time of the specimen at open circuit potential before polarization.
2. The dissolution kinetics of metastable pits increased as a function of cold rolling. The pit peak current, pit growth time and pit growth rate increased with increasing cold working level.
3. Cold rolling increased the metastable pit radii and pit stability product, so that, the attainment of critical metal cations concentration needed to prevent repassivation were more feasible.
4. The rate of metastable pitting decreased with increasing cold rolling. Dissolution of MnS inclusions of cold rolled specimens during free corrosion potential measurement is believed to decrease available sites for nucleation of metastable pitting. Therefore, the frequency of metastable pitting decreased.
5. The probability of formation of stable pits did not change with cold rolling. Although cold rolling increased the probability of transition from metastability to stability, the reduction of metastable pitting occurrence resulted in almost same distribution of pitting potential.

Acknowledgments

This work was performed under the sponsorship of the Ferdowsi University of Mashhad for postgraduate students.

References

[1] B. Mazza, P. Pedeferri, D. Sinigaglia, A. Cigada, L. Lazzari, G. Re, D. Wenger, Relationship between the electrochemical and corrosion behavior and the

structure of stainless steels subjected to cold plastic deformation, J. Electrochem. Soc. 123 (1976) 1157–1163.
[2] A. Barbucci, G. Cerisola, P.L. Cabot, Effect of cold-working in the passive behavior of 304 stainless steel in sulfate media, J. Electrochem. Soc. 149 (2002) B534–B542.
[3] L. Peguet, B. Malki, B. Baroux, Influence of cold working on the pitting corrosion resistance of stainless steels, Corros. Sci. 49 (2007) 1933–1948.
[4] Y. Lü, B. Hutchinson, D.A. Molodov, G. Gottstein, Effect of deformation and annealing on the formation and reversion of ε-martensite in an Fe–Mn–C alloy, Acta Mater. 58 (2010) 3079–3090.
[5] B. Mazza, P. Pedeferri, D. Sinigaglia, A. Cigada, G. Fumagalli, G. Re, Electrochemical and corrosion behaviour of work-hardened commercial austenitic stainless steels in acid solutions, Corros. Sci. 19 (1979) 907–921.
[6] N. Parvathavarthini, R.K. Dayal, J.B. Gnanamoorthy, Influence of prior deformation on the sensitization of AISI Type 316LN stainless steel, J. Nucl. Mater. 208 (1994) 251–258.
[7] S.V. Phadnis, A.K. Satpati, K.P. Muthe, J.C. Vyas, R.I. Sundaresan, Comparison of rolled and heat treated SS304 in chloride solution using electrochemical and XPS techniques, Corros. Sci. 45 (2003) 2467–2483.
[8] A.K. Roy, S. Bandyopadhyay, S.B. Suresh, D. Maitra, P. Kumar, D. Wells, L. Ma, Relationship of residual stress to dislocation density in cold-worked martensitic alloy, Mater. Sci. Eng. A 416 (2006) 134–138.
[9] J.H. Russell, B.S. Covino, J.W. Simmons, The Effect of Cold Working on the Sensitization of a High Nitrogen Stainless Steel, NACE International, Denver, Co, 1996.
[10] R. Štefec, F. Franz, A study of the pitting corrosion of cold-worked stainless steel, Corros. Sci. 18 (1978) 161–168.
[11] V. Vignal, R. Oltra, C. Josse, Local analysis of the mechanical behaviour of inclusions-containing stainless steels under straining conditions, Scripta Mater. 49 (2003) 779–784.
[12] H.-L. Yu, X.-H. Liu, H.-Y. Bi, L.-Q. Chen, Deformation behavior of inclusions in stainless steel strips during multi-pass cold rolling, J. Mater. Process. Technol. 209 (2009) 455–461.
[13] T. Shibata, Stochastic studies of passivity breakdown, Corros. Sci. 31 (1990) 413–423.
[14] T. Shibata, W.R. Whitney award lecture: statistical and stochastic approaches to localized corrosion, Corrosion 52 (1996) (1996) 813–830.
[15] T. Cassagne, M. Bonis, C. Duret, J.L. Crolet, Limitations of PH metallurgical mechanical and corrosion aspects, in: Corrosion 2003, NACE International, San Diego, CA, 2003.
[16] C.N. Hsiao, C.S. Chiou, J.R. Yang, Aging reactions in a 17-4 PH stainless steel, Mater. Chem. Phys. 74 (2002) 134–142.
[17] M. Murayama, K. Hono, Y. Katayama, Microstructural evolution in a 17-4 PH stainless steel after aging at 400 °C, Metall. Trans. A 30 (1999) 345–353.
[18] M.R.T. Shoushtari, M.H. Moayed, A. Davoodi, Galvanic corrosion of gas tungsten arc repair welds in 17-4PH stainless steel in 3·5% NaCl solution, Corros. Eng. Sci. Tech. 46 (2011) 406–414.
[19] M.R.T. Shoushtari, M.H. Moayed, A. Davoodi, Post-weld heat treatment influence on galvanic corrosion of GTAW of 17-4PH stainless steel in 3·5%NaCl, Corros. Eng. Sci. Tech. 46 (2011) 415–424.
[20] H.C. ASM International, ASM Handbook, vol. 9, ASM International, Materials Park, OH, 2004.
[21] S.S.M. Tavares, F.J. da Silva, C. Scandian, G.F. da Silva, H.F.G. de Abreu, Microstructure and intergranular corrosion resistance of UNS S17400 (17-4PH) stainless steel, Corros. Sci. 52 (2010) 3835–3839.
[22] K. Darowicki, S. Krakowiak, The current threshold value in potentiodynamic determination of the breakdown potential, Electrochim. Acta 42 (1997) 2559–2562.
[23] C. Lemaitre, A. Abdel Moneim, R. Djoudjou, B. Baroux, G. Beranger, A statistical study of the role of molybdenum in the pitting resistance of stainless steels, Corros. Sci. 34 (1993) 1913–1922.
[24] G. Salvago, G. Fumagalli, Application of breakdown potential distribution in corrosion comparisons of stainless steels, Corrosion 52 (1996) 760–767.
[25] P.C. Pistorius, G.T. Burstein, Metastable pitting corrosion of stainless steel and the transition to stability, Philos. Trans. R. Soc. Lond. A 341 (1992) 531–559.
[26] G.S. Frankel, L. Stockert, F. Hunkeler, H. Boehni, Metastable pitting of stainless steel, Corrosion 43 (1987) 429–436.
[27] M.H. Moayed, R.C. Newman, Evolution of current transients and morphology of metastable and stable pitting on stainless steel near the critical pitting temperature, Corros. Sci. 48 (2006) 1004–1018.
[28] Y. Kim, R.G. Buchheit, A characterization of the inhibiting effect of Cu on metastable pitting in dilute Al–Cu solid solution alloys, Electrochim. Acta 52 (2007) 2437–2446.
[29] J.R. Galvele, Transport processes and the mechanism of pitting of metals, J. Electrochem. Soc. 123 (1976) 464–474.
[30] G.O. Ilevbare, G.T. Burstein, The role of alloyed molybdenum in the inhibition of pitting corrosion in stainless steels, Corros. Sci. 43 (2001) 485–513.
[31] M.H. Moayed, R.C. Newman, The relationship between pit chemistry and pit geometry near the critical pitting temperature, J. Electrochem. Soc. 153 (2006) B330–B335.
[32] T. Shibata, T. Takeyama, Stochastic theory of pitting corrosion, Corrosion 33 (1977) 243–251.
[33] N.J. Laycock, M.H. Moayed, R.C. Newman, Metastable pitting and the critical pitting temperature, J. Electrochem. Soc. 145 (1998) 2622–2628.
[34] P.C. Pistorius, G.T. Burstein, Aspects of the effects of electrolyte composition on the occurrence of metastable pitting on stainless steel, Corros. Sci. 36 (1994) 525–538.
[35] K.H. Lo, C.H. Shek, J.K.L. Lai, Recent developments in stainless steels, Mater. Sci. Eng. R 65 (2009) 39–104.
[36] B. Ravi Kumar, R. Singh, B. Mahato, P.K. De, N.R. Bandyopadhyay, D.K. Bhattacharya, Effect of texture on corrosion behavior of AISI 304L stainless steel, Mater. Charact. 54 (2005) 141–147.
[37] A. Barbucci, M. Delucchi, M. Panizza, M. Sacco, G. Cerisola, Electrochemical and corrosion behaviour of cold rolled AISI 301 in 1 M H_2SO_4, J. Alloys Compd. 317–318 (2001) 607–611.
[38] F. Christien, M.T.F. Telling, K.S. Knight, Neutron diffraction in situ monitoring of the dislocation density during martensitic transformation in a stainless steel, Scripta Mater. 68 (2013) 506–509.
[39] G.S. Eklund, Initiation of pitting at sulfide inclusions in stainless steel, J. Electrochem. Soc. 121 (1974) 467–473.
[40] M.A. Baker, J.E. Castle, The initiation of pitting corrosion at MnS inclusions, Corros. Sci. 34 (1993) 667–682.
[41] H. Krawiec, V. Vignal, O. Heintz, R. Oltra, Influence of the dissolution of MnS inclusions under free corrosion and potentiostatic conditions on the composition of passive films and the electrochemical behaviour of stainless steels, Electrochim. Acta 51 (2006) 3235–3243.
[42] J. Stewart, D.E. Williams, The initiation of pitting corrosion on austenitic stainless steel: on the role and importance of sulphide inclusions, Corros. Sci. 33 (1992) 457–474.
[43] T.L.S.L. Wijesinghe, D.J. Blackwood, Real time pit initiation studies on stainless steels: the effect of sulphide inclusions, Corros. Sci. 49 (2007) 1755–1764.
[44] D.E. Williams, C. Westcott, M. Fleischmann, Stochastic models of pitting corrosion of stainless steels, J. Electrochem. Soc. 132 (1985) 1796–1804.
[45] D.E. Williams, J. Stewart, P.H. Balkwill, The nucleation, growth and stability of micropits in stainless steel, Corros. Sci. 36 (1994) 1213–1235.